

WO 2005/017148

PCT/US2003/041600

Fig. 3

SDS-PAGE Analysis of
2H7 scFvIgG1 (SSS-S)H WCH2 WCH3 Protein.

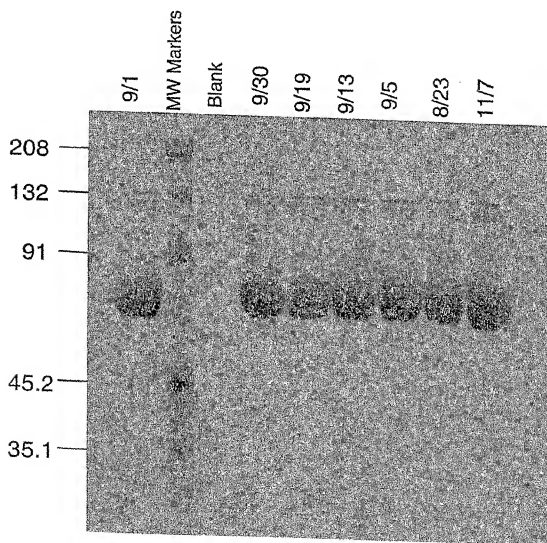


Fig. 4A

Complement Mediated B Cell Killing After Binding of
CD20-targeted 2H7 scFvIgG1 (SSS-S)H WCH2 WCH3:

2H7scFv-Ig Concentration	RAMOS		BJAB	
	# live cells/total cells		# live cells/total cells	
20 µg/ml + complement	-	0.16	-	0.07
5 µg/ml + complement	-	0.2	-	N.D.
1.25 µg/ml + complement	-	0.32	-	0.1
Complement alone	-	0.98	-	0.94

*Viability was determined by trypan blue exclusion and is tabulated as the fraction of viable cells out of the total number of cells counted.

**N.D. (not determined).

Fig. 4B

Antibody-dependent cellular cytotoxicity (ADCC) mediated by 2H7scFv-IgG1
(SSS-S)H WCH2 WCH3:

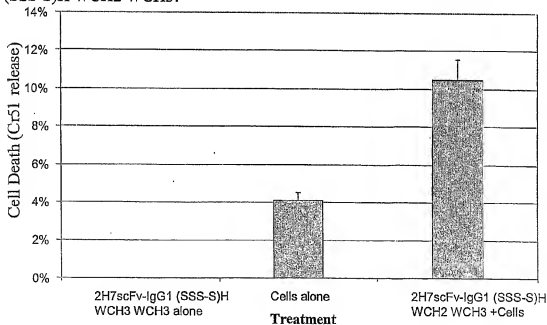


Fig. 5

Effects of Crosslinking of CD20 and CD40 Cell Surface Receptors
on B Cell Proliferation:

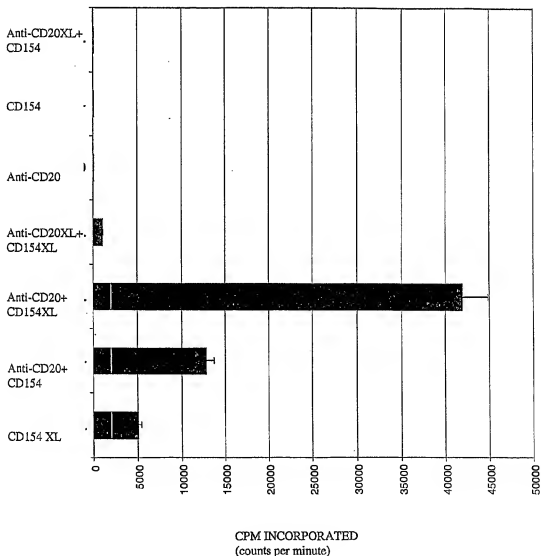


Fig. 6

Effect of Simultaneous ligation of CD20 and CD40
on CD95 and apoptosis.

Fig. 6A.

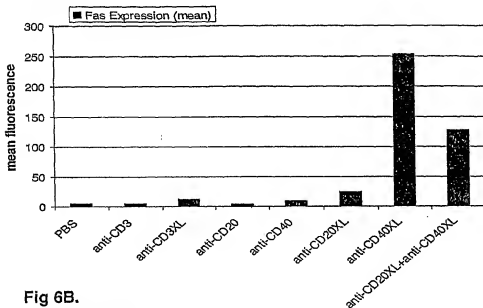
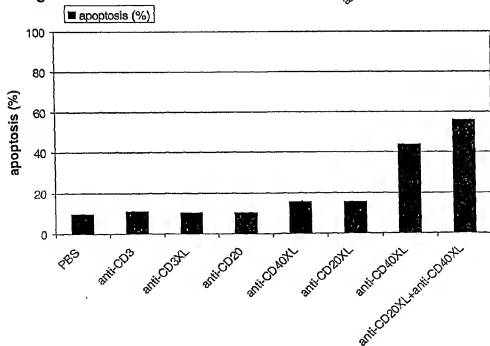


Fig 6B.



Stimuli

Fig. 7A

2H7-CD154 L2 cDNA and predicted amino acid sequence:

```

HindIII      NcoI  2H7 VL Leader Peptide →
~~~~~      ~~~~~
1  AAGCTTGGCCG CC  ATGGATT TCAAGTGCAG ATTTTCAGCT TCCTGCTAAT CAGTGCTTCA

                                2H7 VL →
51  V I I A R G Q I V L S Q S P A I L S A S
    GTCATAATTG CCAGAGGACA AATTGTTCTC TCCAGTCTC CAGCAATCCT GTCTGCATCT

    P G E K V T M T C R A S S S V S Y M H W
121  CCAGGGGAGA AGGTCACAAT GACTTGCAGG GCCAGCTCAA GTGTAAGTTA CATGCACTGG

                                BamHI
                                ~~~~~
181  Y Q Q K P G S S P K P W I Y A P S N L A
    TACCAGCAGA AGCCAGGATC TCCTCCCAA CCTCGATT ATGCCCCATC CAACCTGGCT

    S G V P A R F S G S G S G T S Y S L T I
241  TCTGAGTCC CTGCTCGCTT CAGTGGCAGT GGGTCTGGGA CCTCTACTC TCTACAATC

    S R V E A E D A A T Y Y C Q Q W S F N P
301  AGCAGAGTGG AGGCTGAAGA TGCTGCCACT TATTACTGCC AGCAGTGGAG TTTTAACCCA

(Gly2Ser)3 Linker →
P T F G A G T K L E L K G G G G S G G G
361  CCCACGTTCG GTGCTGGGAC CAAGCTGGAG CTGAAAGGTG CCGGTGGCTC GGGCGGTGGT

                                2H7 VH →
421  G S G G G G S S Q A Y L Q Q S G A E L V
    GGATCTGAG GAGTGGGAG CTCTCAGGCT TATCTACAGC AGTCTGGGTC TGAGCTGGTG

    R P G A S V K M S C K A S G Y T F T S Y
481  AGGCCGSGG CCTCAGTGAA GATGTCCTGC AAGGCTTCTG GCTACACATT TACCAGTTAC

    N M H W V K Q T P R Q G L E W I G A I Y
541  AATATGCACT GGGTAAGCA GACACCTAGA CAGGCGCTGG AATGGATTGG AGCTATTATT

    P G N G D T S Y N Q K F K G K A T L T V
601  CCAGGAATG GTGATACTTC CTACAATCAG AAGTTCAAGG GCAAGCCAC ACTGACTGTA

    D K S S S T A Y M Q L S S L T S E D S A
661  GACAAATCCT CCAGCACAGC CTACATGCAG CTCAGCAGCC TGACATCTGA AGACTCTGGC

    V Y F C A R V V Y Y S N S Y W Y F D V W
721  GTCTATTCTT GTGCAAGAGT GGTGTAATAT AGTAACCTTT ACTGGTACTT CGATGCTGGG
  
```

Fig. 7A (continued)

human CD154/amino acid 48→

Bcl/Bam hybrid site

781 G T G T T V T V S D P R R L D K I E D E
GGCACAGGA CCACGGTCAC CGTCTCTGAT CCAAGAAGGT TGGACAAGAT AGAAGATGAA

BclI

841 R N L H E D F V F M K T I Q R C N T G E
AGGAATCTTC ATGAAGATTT TGTATTCATG AAAACGATAC AGAGATGCAA CACAGGAGAA

BclI

901 R S L S L L N C E E I K S Q F E G F V K
AGATCCTTAT CCTTACTGAA CTGTGAGGAG ATTAAAAGCC AGTTTGAAGG CTTTGTGAAG

BclI

961 D I M L N K E E T K K E N S F E M Q K G
GATATAATGT TAAACAAAGA GGAGACGAAG AAAGAAACA GCTTTGAAAT GCAAAAAGGT

BclI

1021 D Q N P Q I A A H V I S E A S S K T T S
GATCAGATC CTCAAATTGC GGCACATGTC ATAAGTGAGG CCAGCAGTAA AACACATCT

BclI

1081 V L Q W A E K G Y Y T M S N N L V T L E
GTGTTACAGT GGGCTGAAAA AGGATACTAC ACCATGAGCA ACAACTTGGT AACCCGGA

BclI

1141 N G K Q L T V K R Q G L Y Y I Y A Q V T
AATGGGAAAC AGCTGACCGT TAAAAGACAA GGACTCTATT ATATCTATGC CCAAGTCACC

HindIII

1201 F C S N R E A S S Q A P F I A S L C L K
TTCTGTGCA ATCGGGAAGC TTCGAGTCAA GCTCCATTTA TAGCCAGCCT CTGCTTAAAG

HindIII

1261 S P G R F E R I L L R A A N T H S S A K
TCCCCGGTA GATTCGAGAG AATCTTACTC AGAGCTGCAA ATACCCACAG TTCGCGCAAA

HindIII

1321 P C G Q Q S I H L G G V F E L Q P G A S
CCTTGCGGGC AACAAATCCAT TCACTTGGGA GGAGTATTG AATTGCAACC AGGTGCTTGC

NcoI

1381 V F V N V T D P S Q V S H G T G F T S F
GTGTTTGCA ATGTGACTGA TCCAAGCCAA GTGAGCCATG GCAGTGCCCT CAGTCCTTT

XhoI XbaI

1441 G L L K L E * * S R
GGCTTACTCA AACTCGAGTG ATAATCTAGA

WO 2005/017148

ECT/US2003/041600

Fig. 7B.

2H7scFv-CD154 S4 cDNA and predicted amino acid sequence:

```

HindIII      NcoI
~~~~~      ~~~~~
                2H7 VL Leader Peptide→
1  AAGCTTGCCG CC  ATGGATT TCAAGTCAG ATTTTCAGCT TCCTGCTAAT CAGTGCTTCA

                2H7 VL →
61  V I I A R G Q I V L S Q S P A I L S A S
    GTCATAATTG CCAGAGGACA AATTGTTCTC TCCCAGTCTC CAGCAATCCT GTCTGCATCT

    P G E K V T M T C R A S S S V S Y M H W
121 CCAGGGGAGA AGGTACAAT GACTTGCAAG GCCAGCTCAA GTGTAAGTTA CATGCACCTGG

                BamHI
                ~~~~~
181  Y Q Q K P G S S P K P W I Y A P S N L A
    TACCAGCAGA AGCCAGGATC CTCCCCCAA CCCTGGATT ATGCCCATC CAACCTGGCT

    S G V P A R F S G S G S G T S Y S L T I
241 TCTGAGTCC GCTCTCGCTT CAGTGGCAGT GGTCTGGGA CCTCTACTC TCTCAATAC

    S R V E A E D A A T Y Y C Q Q W S F N P
301 AGCAGAGTGG AGGCTGAAGA TGCTGCCACT TATTACTGCC AGCAGTGGAG TTTTAACCCA

(Gly,Ser)3 Linker →
361  P T P G A G T K L E L K G G G G S G G G
    CCCACGTTG GTGCTGGGAC CAAGCTGGAG CTGAAAGGTG CGGTGGGCTC GGGCGGTGGT

                2H7 VH →
421  G S G G G G S S Q A Y L Q Q S G A E L V
    GGATCTGGAG GAGTGGGAG CTCTCAGGCT TATCTACAGC AGTCTGGGCG TGAGCTGGTG

    R P G A S V K M S C K A S G Y T F T S Y
481 AGGCCTGGGG CCTCAGTGA GATGTCTGCG AAGGCTTCTG GCTACACATT TACCAGTTAC

    N M H W V K Q T P R Q G L E W I G A I Y
541 AATATGCACT GGGTAAAGCA GACACCTAGA CAGGGCCTGG AATGGATTGG AGCTATTATT

    P G N G D T S Y N Q K F K G K A T L T V
601 CCAGGAATAG GTGATACTTC CTACAATCAG AAGTCAAGG GCAAGGCCAC ACTGACTGTA

    D K S S S T A Y M Q L S S L T S E D S A
661 GACAAATCCT CCAGCACAGC CTACATGCAG CTCAGCAGCC TGACATCTGA AGACTCTGGC

    V Y F C A R V V Y Y S N S Y W Y F D V W
721 GTCTATTCTT GTGCAAGAGT GGTGTACTAT AGTAACTCTT ACTGGTACTT CGATGCTGCG
  
```

WO 2005/017148

PCT/US2003/041600

Fig. 7B

human CD154/amino acid 108 →

Bcl/Bam hybrid site

BclI
G T G T T V T V S D P E N S F E M Q K G
781 GGCACAGGGA CCACGGTCAC CGTCTCTGAT CCAGAAAACA GCTTTGAAAT GCAAAAAGGT

BclI
~~~~~  
D Q N P Q I A A H V I S E A S S K T T S  
841 GATCAGAATC CTCAAATGCG GCACATGTC ATAAAGTGAGG CCAGCAGTAA AACACATCT

V L Q W A E K G Y Y T M S N N L V T L E  
901 GTGTTACAGT GGGCTGAAAA AGGATACTAC ACCATGAGCA ACAACTTGGT AACCTGGAA

N G K Q L T V K R Q G L Y Y I Y A Q V T  
961 AATGGGAAC AGCTGACCGT TAAAAGACAA GGACTCTATT ATATCTATGC CCAAGTCACC

HindIII  
~~~~~  
F C S N R E A S S Q A P F I A S L C L K
1021 TTCTGTTCCTA ATCGGGAAGC TTCGAGTCAA GCTCCATTTA TAGCCAGCCT CTGCCTAAAG

S P G R F E R I L L R A A N T H S S A K
1081 TCCCCCGGTA GATTCGAGAG AATCTTACTC AGAGCTGCAA ATACCACAG TTCCGCCAAA

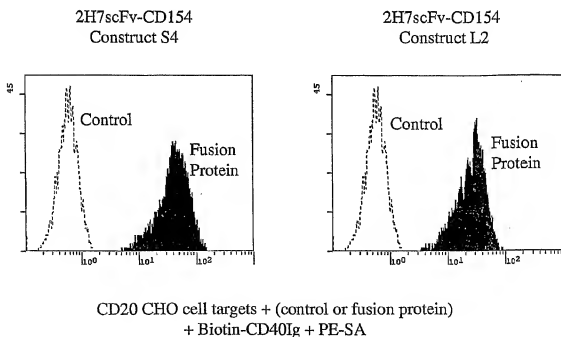
P C G Q Q S I H L G G V F E L Q P G A S
1141 CCTTGCGGGC AACAAATCCAT TCACTTGGGA GGAGTATTTG AATTGCAACC AGGTGCTTCG

NcoI
~~~~~  
V F V N V T D P S Q V S H G T G F T S F  
1201 GTGTTTGTCA ATGTGACTGA TCCAAGCCAA GTGAGCCATG GCATGGCTT CAGTCCCTTT

XhoI XbaI  
~~~~~  
G L L K L E * * S R
1261 GGCTTACTCA AACTCGAGTG ATAACTTAGA

Fig. 8

Simultaneous Binding of 2H7scFv-CD154
Fusion Proteins to CD20 and CD40

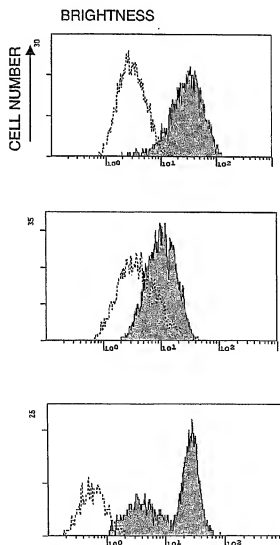


WO 2005/017148

PCT/US2003/041600

Fig. 9

Induction of Apoptosis Measured by Binding of Annexin V after incubation with 2H7scFv-CD154



.....control supernatant — 2H7scFv-CD154 supernatant

Fig. 10

Proliferation of T51 B Cell Line After Incubation with 2H7
scFv-CD154 S4 or 2H7 scFv-CD154 L2 Constructs

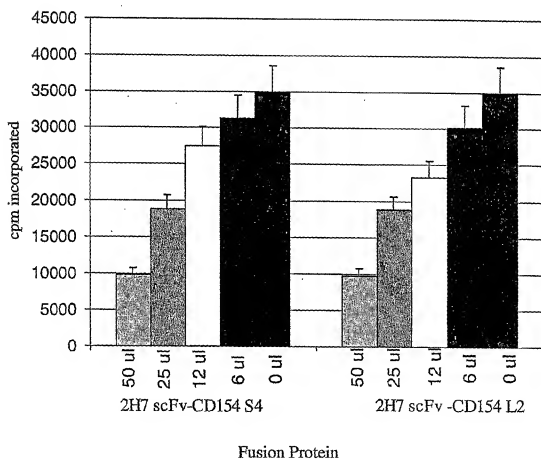
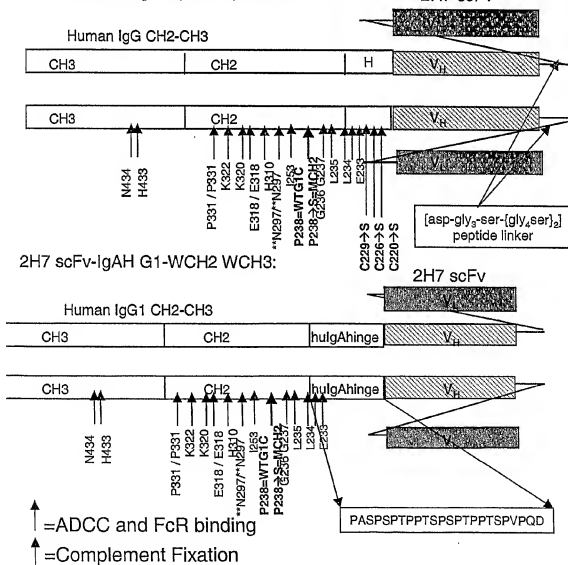


Fig. 11

Schematic Representation of 2H7 scFvIg Constructs

2H7 scFvIgG (SSS-S)H WCH2 WCH3

OR 2H7 scFvIgG1 (SSS-S)H P238SCH2 WCH3 : 2H7 scFv



WO 2005/017148

PCT/US2003/041600

Fig. 12

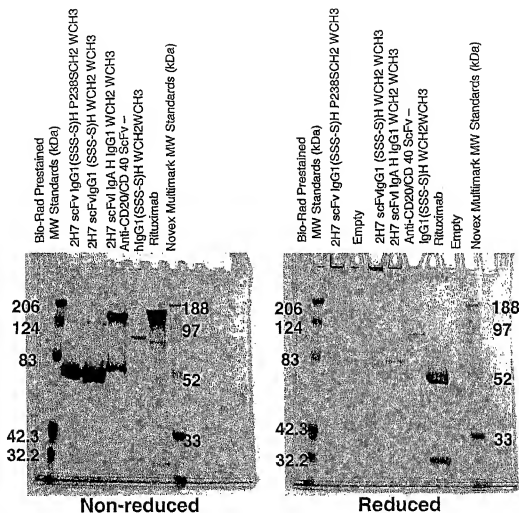


Figure 12: SDS-PAGE Analysis of CytosB Derivatives. Purified fusion protein derivatives of CytosB-scFvIg molecules and Rituximab were resuspended SDS sample buffer, boiled, loaded onto 10% Novex Tris-Bis gels (Invitrogen, San Diego, CA) and subjected to nonreducing (left panel) or reducing (right panel) SDS-PAGE electrophoresis at 175 volts. Two different molecular weight markers, BioRad prestained markers, and Novex Multimark molecular weight markers were also loaded onto each gel and the approximate size in kDa of each marker band is indicated along each side of the photographed gels. Gels were stained in Coomassie Blue stain and photographed with a SONY Mavica Digital camera. The mutant hinge forms of 2H7 scFvIgG1 migrate at approximately 70 kDa under both nonreducing and reducing conditions, indicating that these molecules are monomeric rather than dimeric in structure. The IgA hinge form of 2H7scFvIg migrates at approximately 75 kDa under reducing conditions, but migrates predominately as a dimer of 140 kDa with a fraction of the protein migrating at 75 kDa under nonreducing conditions. Under nonreducing conditions, rituximab migrates as a diffuse band of between 150 and 200 kDa. The heavy and light chains resolve into separate bands of approximately 32 and 50 kDa when rituximab is reduced and subjected to SDS-PAGE.

Fig. 13

ADCC Activity of CytoxB (2H7 scFvIg) Constructs.

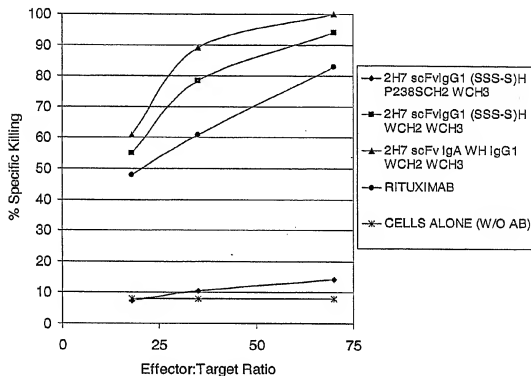


Figure 13: ADCC Activity of CytoxB Derivatives Compared to Rituximab. ADCC activity of CytoxB Derivatives or Rituximab was measured *in vitro* against BJAB B lymphoma cell line as target and using fresh human PBMC as effector cells. Effector to target ratios were varied as follows: 70:1, 35:1, and 18:1, with the number of BJAB cells per well remaining constant but varying the number of PBMC. Bjab cells were labeled for 2 hours with ^{51}Cr and aliquoted at a cell density of 5×10^4 cells/well to each well of flat-bottom 96 well plates. Purified fusion proteins or rituximab were added at a concentration of 10 mg/ml, and PBMC were added at 9×10^5 cells/well (18:1), 1.8×10^6 cells/well (35:1), or 3.6×10^6 cells/well (70:1), in a final volume of 200 μl . Spontaneous release was measured without addition of PBMC or fusion protein, and maximal release was measured by the addition of detergent (1% NP-40) to the appropriate wells. Reactions were incubated for 4 hours, and 100 μl culture supernatant harvested to a Lumaplate (Packard Instruments) and allowed to dry overnight prior to counting cpm released on a Packard Top Count NXT Microplate Scintillation Counter.

Fig. 14

CDC of Cytos B (2H7 scFvIg) Constructs

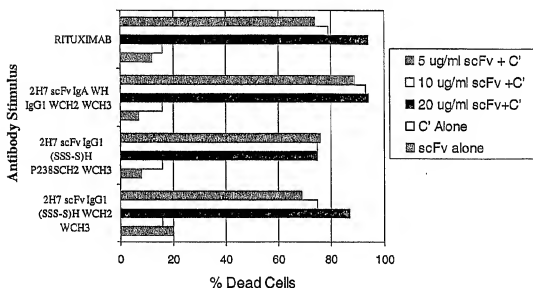
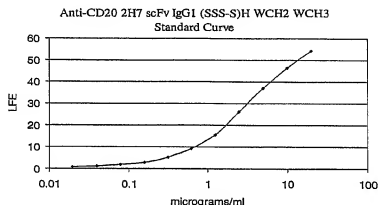


Figure 14: Complement Dependent Cytotoxicity (CDC) Activity of CytosB Derivatives Compared to Rituximab. 2H7 scFvIgG1 (SSS-S)H WCH2 WCH3, 2H7 scFvIgG1 (SSS-S)H WCH2 WCH3, and 2H7scFv IgA WH IgG1 WCH2 WCH3 derivatives and Rituximab were compared for their ability to mediate complement dependent cytotoxicity. Rabbit complement (Pel-Freez) was diluted 1:10 and added to BJAB cells along with dilutions of each antibody derivative (20 μ g/ml, 10 μ g/ml, and 5 μ g/ml). Controls were also included without addition of complement (C') or scFv derivative. Reactions were allowed to continue for 1 hour, and cells from each well were then stained with trypan blue and the cell viability counted using a hemacytometer. Data is graphed as % of dead cells/total cells counted for each condition assayed.

Fig. 15

2H7 (anti-CD20) scFv IgG1 (SSS-S)H WCH2 WCH3
In Vivo Half Life



Macaque A99314

Day	Binding intensity (LFE) @ 1:50 dilution of serum	estimated concentration (µg/ml)
Injection #1 → -7	0.213	<0.1
0	0.227	<0.1
1	7.79	25.1
3	5.51	15.6
Injection #2 → 7	3.37	9.4
8	11.33	41.7
10	5.45	15.4
14	0.27	<0.1

Macaque F98081

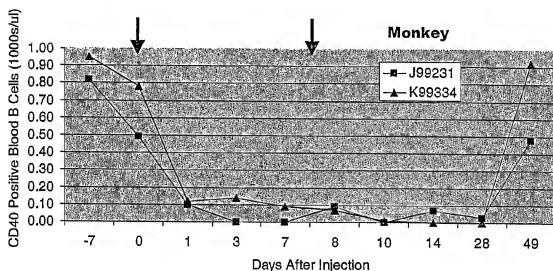
Day	Binding intensity (LFE) @ 1:50 dilution of serum	estimated concentration (µg/ml)
Injection #1 → -7	0.208	<0.1
0	0.219	<0.1
1	6.73	21.9
3	6.14	19.3
Injection #2 → 7	3.04	8.7
8	9.83	33.8
10	4.77	14.4
14	0.231	<0.1

WO 2005/017148

PCT/US2003/041600

Fig. 16

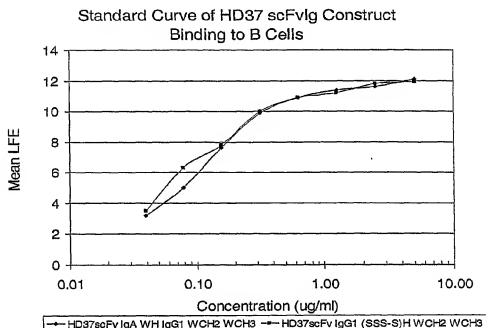
B Cell Depletion in macaques mediated by Cytos B20
(2H7 scFv IgG1 (SSS-S)H WCH2 WCH3) Construct



- CytosB20 injections of 6mg/kg yields 3 week B-cell depletion
- 3-4 day half-life *in vivo*
- CD20 saturation in lymph node B-cells at d14
- No first dose effects
- No anti-chimeric antibody development

Fig. 17

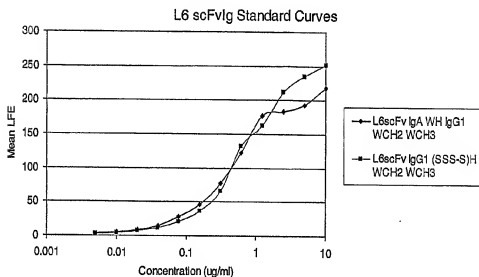
Production Levels of HD37 scFvIg Constructs by CHO Cell Lines



Clone/Isolate	Mean LFE at 1:100	Estimated Concentration
Bulk HD37 scFv		
IgA WH IgG1 WCH2 WCH3	11.2	> 60 ug/ml
1B2	10.4	>50 ug/ml
6C5	10.5	>50 ug/ml
4B1	8.6	>40 ug/ml
Bulk HD37 scFv		
IgG1 (SSS-S)H WCH2 WCH3	10.9	> 50 ug/ml
2G8	10.6	> 50 ug/ml
3F3	8.3	>40 ug/ml
3D9	11.1	> 60 ug/ml

Fig. 18

Production of L6 scFvIg constructs by CHO Cells



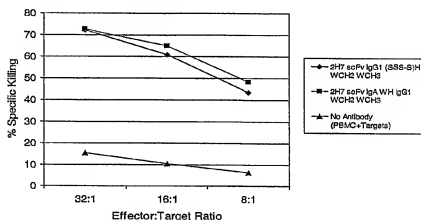
Construct	Mean LFE 1:20	Estimated Concentration
L6scFv IgA WH IgG1 WCH2 WCH3 unamplified CHO sup	51.1	6.25 ug/ml
L6scFv IgG1(SSS-S)H WCH2 WCH3 unamplified CHO sup	23.0	3.2 ug/ml

Fig. 19

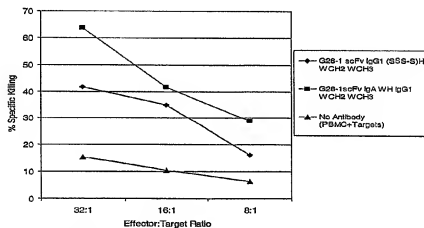
ADCC Activity of 2H7 scFvIg, G28-1 scFvIg, and HD37 scFvIg Constructs

ADCC Activity of scFvs Targeted to B Cell Antigens

A. 2H7 (anti-CD20) scFv constructs



B. G28-1 (anti-CD37) scFv constructs



C. HD37 (anti-CD19) scFv constructs

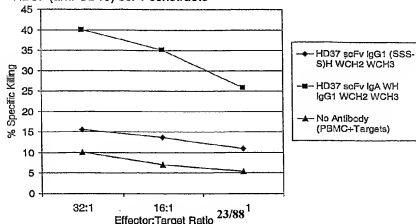


Fig. 20

ADCC Activity of L6 scFvIg Constructs

ADCC Activity of L6scFvIg Constructs with 2981 Targets

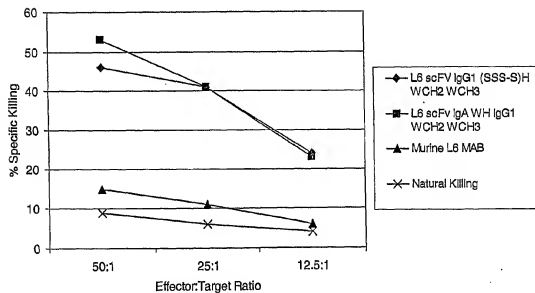


Fig. 21

SDS-PAGE Analysis of L6 and 2H7
scFvIg Fusion Proteins.

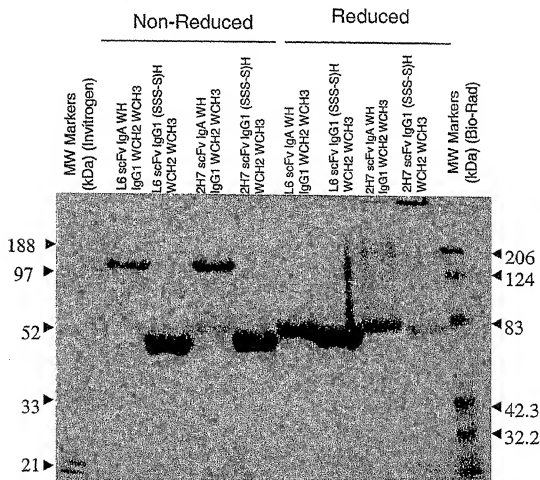


Fig. 22

SDS-PAGE Analysis of G28-1 and HD37
scFvIg Constructs.

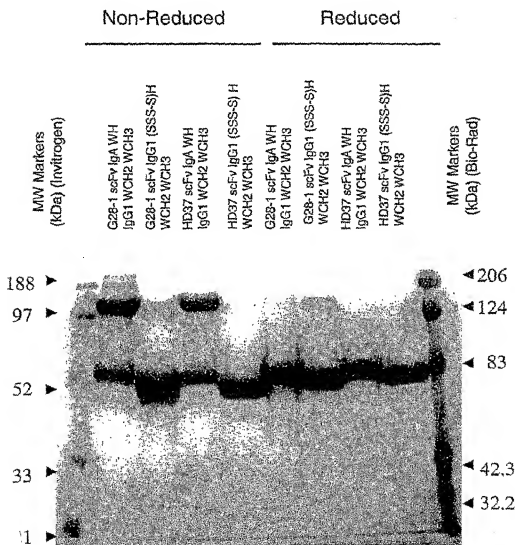


Fig. 23

Sequence alignment of human and llama Fc regions.

	HINGE	CH2→
an IgG1:	DQEPKSCDKT-----HTCPPC	PAPELLGGPSVFLFPPPKPKDTLMISRTPEVTCVVDVSHEDPEVKFNWYVDG
ma IgG2:	DQSPKTPKPQPPQPPNPPTTESKCPKC	PAPELLGGPSVFLFPPPKPDVLSISGRPEVTCVVDVVGQEDPEVFNWYIDG
ma IgG1:	--SPHGG-----CTCPQC	PAPELLGGPSVFPFPPPKPDVLSISGRPEVTCVVDVVGKEDPEVFNWYIDG
ma IgG3:	--AHHSDEPT-----SKCPKC	PGPELLGGPTVFIFPPKAKDVLSTTRKPEVTCMLWTVVKKTLRSSSSSVSD

VEVINAKTKPREEQYNSTYRVVSVLTVLHQDWLNGKEYKCKVSNKALPAPIEKTISKAKGQPREPQVYTLPPSRDELTKNQVSLT
TAEVIRANTRPKKEEQFNSTYRVVSVLPQHQQDWLTKGEFKCKVNNKALPAPIEKTISKAKGQTPREPQVYTLAPHREELAKDTVSVT
VEVRTANTPKKEEQFNSTYRVVSVLPQHQQDWLTKGEFKCKVNNKALPAPIERTISKAKGQTPREPQVYTLAPHREELAKDTVSVT
TEVHTAETPKKEEQFNSTYRVVSVLPQHQQDWLTKGEFKCKVNNKALPAPIERTISKAKGQTPREPQVYTLAPHREELAKDTVSVT

CLVKGFFPSDI AVEWESNGQPEN--NYKTTFPVLDSGFSFLYSKLTVDKSRNQGNVFS CSMHEALHNHYTQKSLSLSPGK
CLVKGFFPPDINVEWQRNGQPESXGTATPPQLDNDGTYFLXSKXSVGKNTWQGGSTPTCVVMHEALHNHYTQKSLTQSSGK
CLVKGFFPADINVEWQRNGQPESBGTANTPPQLDNDGTYFLYSLRSLVGKNTWQGETLTGVVMHEALHNHYTQKSLTQSSGK
CLVKGFFPADINVEWQRNGQPESBGTANTPPQLDNDGTYFLYSLRSLVGKNTWQGEVPTCVVMHEALHNHYTQKSLTQSSGK

Fig. 24

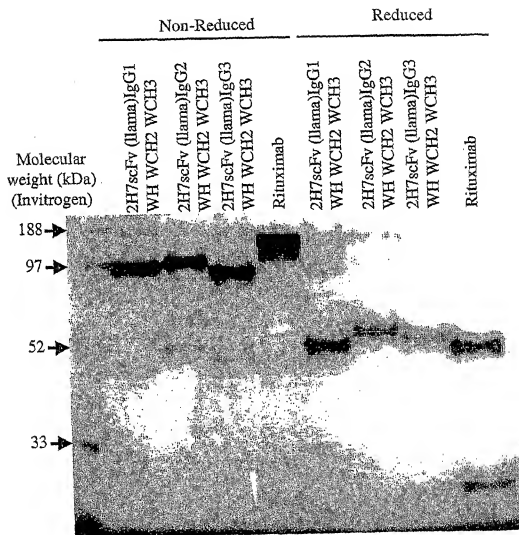


Fig. 25

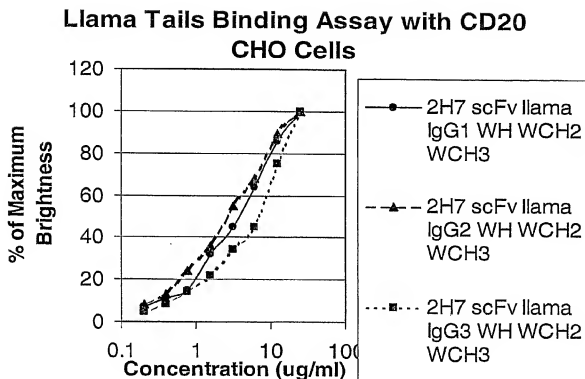


Fig. 26

2H7 scFvIg Llama Tails binding Assay with CD20 CHO Cells

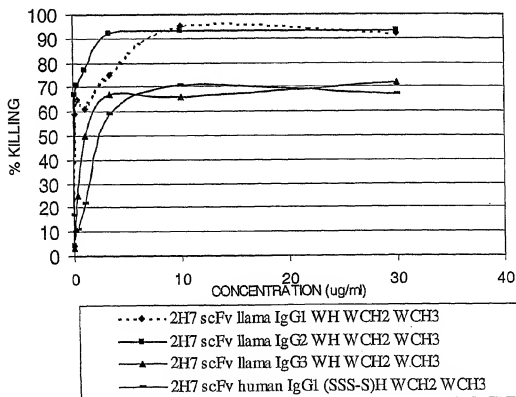


Fig. 27

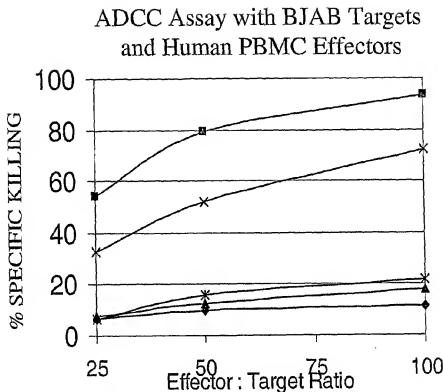


Fig. 28

ADCC Assay with BJAB Cells
And Llama PBMC Effectors

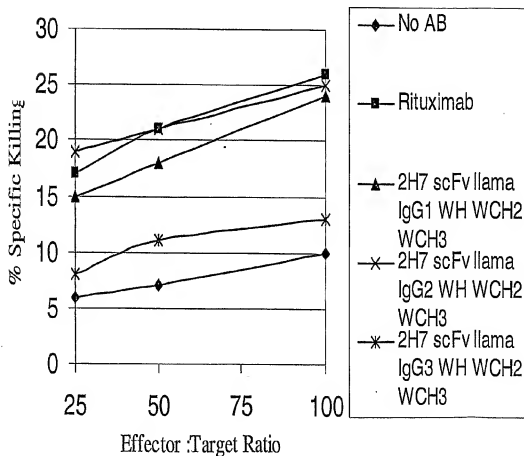


Fig. 29

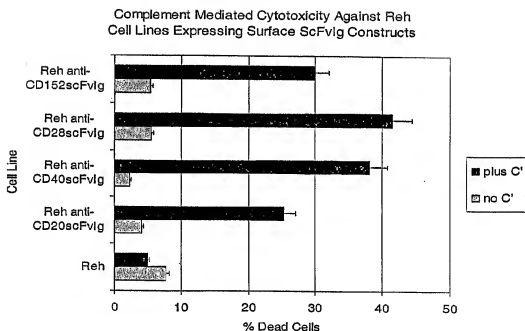


Fig. 30

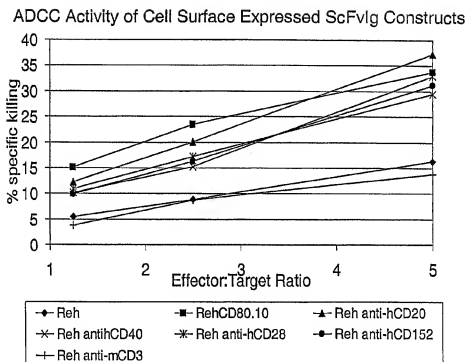


Fig. 31

Ig Constructs and Nomenclature:

Name Identifier	Hinge Sequence	CH2 Sequence	CH3 Sequence
hIgG1 (CCC-P)H WCH2 WCH3	IgG1 WT Hinge (CCC-P)	Wild Type CH2	Wild Type CH3
hIgG1 (SSS-S)H WCH2 WCH3	IgG1 Mutant Hinge (SSS-S)	Wild type CH2 (IgG1)	Wild type CH3 (IgG1)
VH L11S hIgG1 (SSS-S)H WCH2 WCH3	IgG1 Mutant Hinge (SSS-S)	Wild type CH2 (IgG1)	Wild type CH3 (IgG1)
IgG1 (SSC-S)H WCH2 WCH3	IgG1 Mutant Hinge (SSC-S)	Wild type CH2 (IgG1)	Wild type CH3 (IgG1)
IgG1 (SCS-S)H WCH2 WCH3	IgG1 Mutant Hinge (SCS-S)	Wild type CH2 (IgG1)	Wild type CH3 (IgG1)
IgG1 (CSS-S)H WCH2 WCH3	IgG1 Mutant Hinge (CSS-S)	Wild type CH2 (IgG1)	Wild type CH3 (IgG1)
IgG1 (SSS-S)H P238S CH2 WCH3	IgG1 Mutant Hinge (SSS-S)	Mutant CH2 (IgG1) Pro → Ser 238	Wild type CH3 (IgG1)
IgA WH hIgG1 WCH2 WCH3	IgA Hinge	Wild type CH2 (IgG1)	Wild type CH3 (IgG1)
IgA WH IgA WCH2 WCH3	IgA Hinge	Wild type CH2 (IgA)	Wild type CH3 (IgA)
IgA WH IgA WCH2 T4CH3	IgA Hinge	Wild type CH2 (IgA)	Truncated CH3 (IgA) Missing 4 aa at COOH

Fig. 32

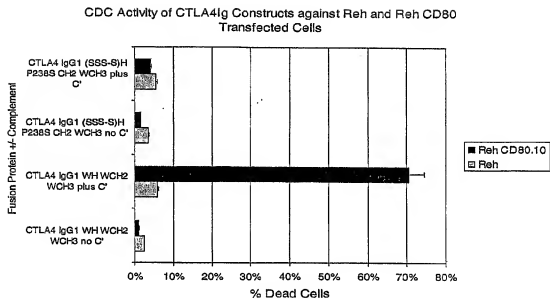
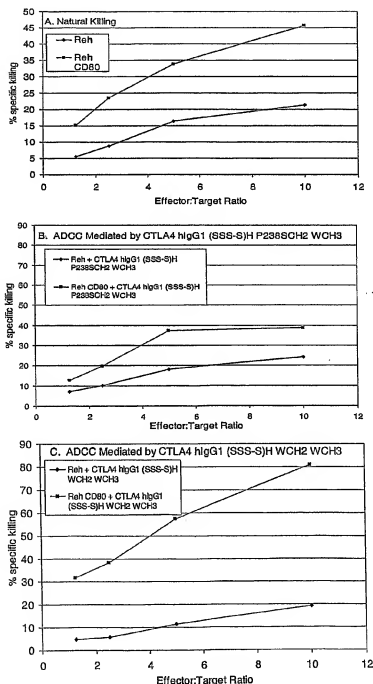


Fig. 33



WO 2005/017148

PCT/US2003/041600

Fig. 34

Binding of 2H7 scFvIg Constructs
with Alternative Tails to CD20 CHO Cells

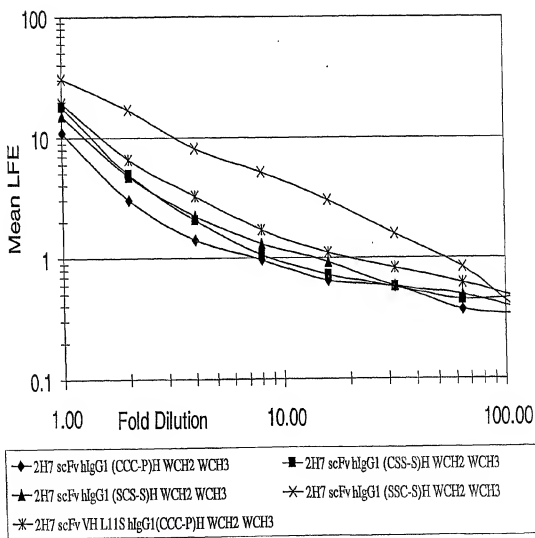


Fig. 35

Immunoblot Analysis of protein immunoprecipitates
from COS transfections of 2H7 scFvIg Constructs

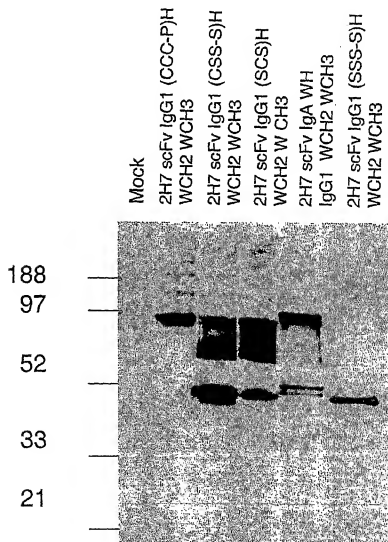


Fig. 36

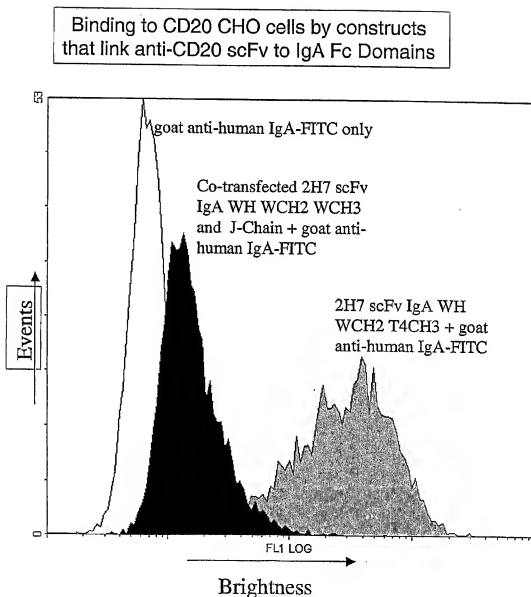


Fig. 37

Titration of CD20 specific scFvIg Constructs
for ADCC Activity Using Whole Blood Effectors

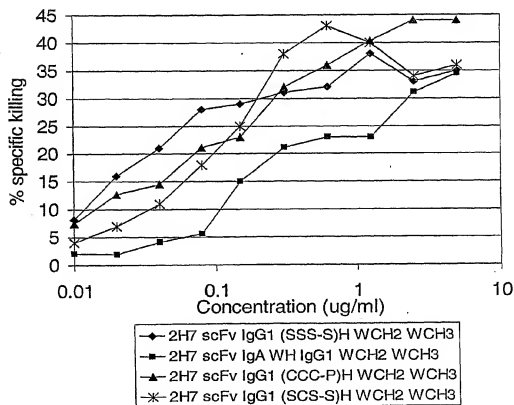


Fig. 38

ADCC Assay of anti-CD20 constructs with alternative tails
(Whole Blood Effectors / BJAB Targets)

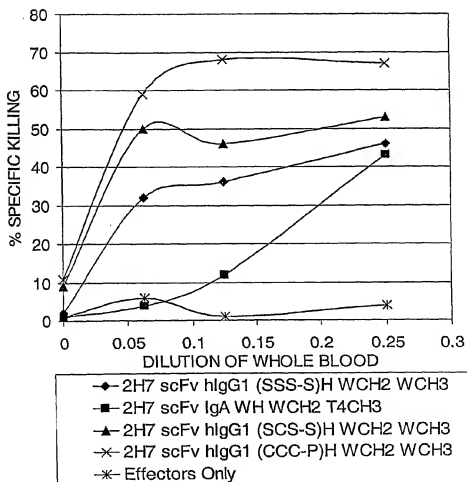
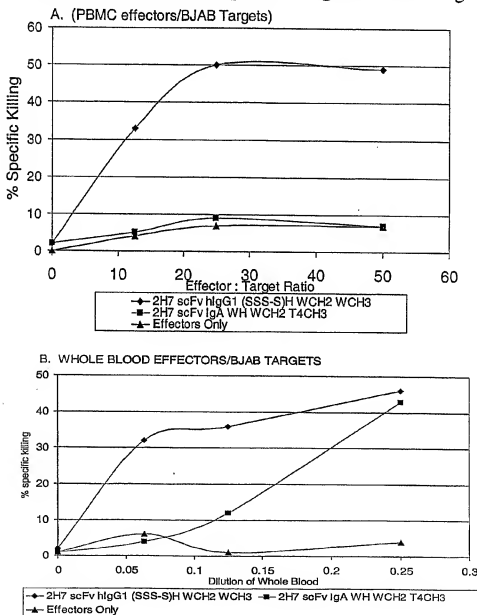


Fig. 39

ADCC Assay of Anti-CD20 scFvIg Constructs
Using Different Effector Populations Against BJAB Targets

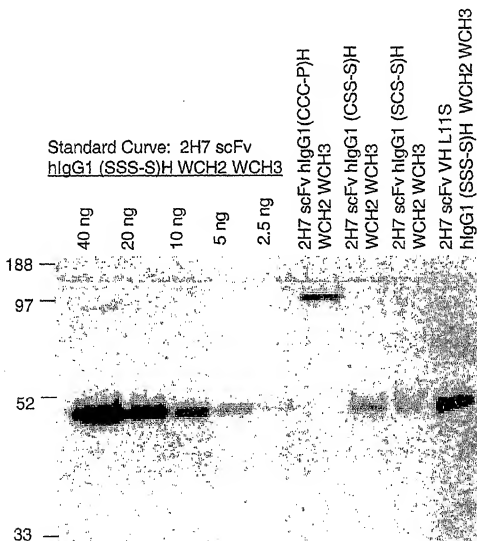


WO 2005/017148

PCT/US2003/041600

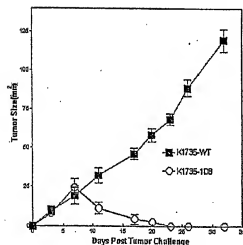
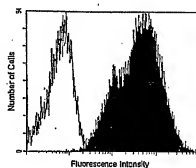
Fig. 40

Immunoblot of 2H7 scFv Ig constructs from COS
Transfections (1 μ l/well) compared to a Concentration Standard

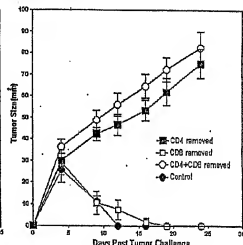


Figures 41A, 41B and 41C

A.



B.



C.

Sheet 45 of 53

Fig. 42

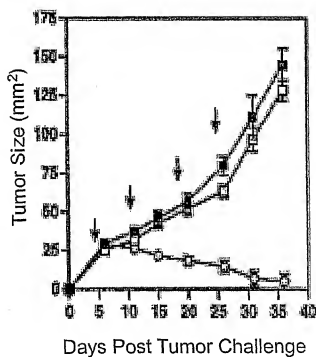
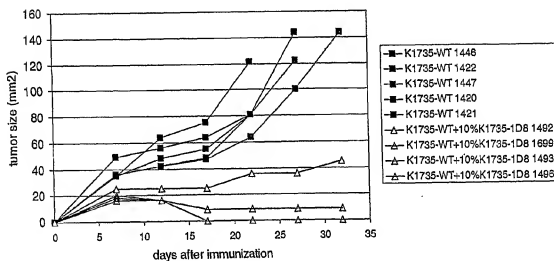


Fig. 43

Mixtures of K1735-WT and K1735-1D8 transfected tumor lines
inhibit tumor outgrowth in C3H mice

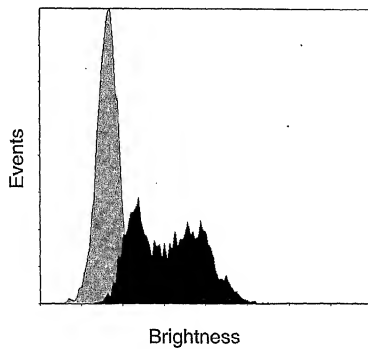


WO 2005/017148

PCT/US2003/041600

Fig. 44

Expression of anti-mouse CD137 (1D8) scFv-hIgG1 (SSS-S)H P238SCH2 WCH3
On the surface of panned Ag104-1D8 Transfected Tumor Cells



WO 2005/017148

PCT/US2003/041600

Fig. 45

Coomassie Stained SDS-PAGE Gel of 2H7 scFv Ig
Constructs

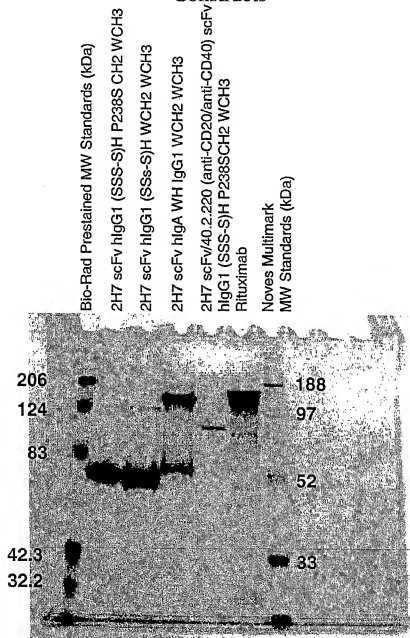
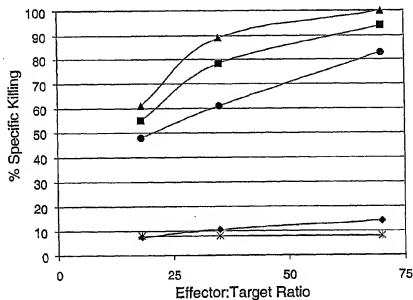


Fig. 46

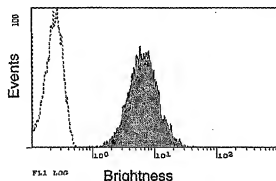
ADCC mediated by 2H7 scFvIg Constructs by human
PBMC effector cells against Bjab targets



- ◆ 2H7 scFv hlgG1 (SSS-S)H P238SCH2 WCH3
- ▲ 2H7 scFv hlgA WH IgG1 WCH2 WCH3
- 2H7 scFv hlgG1 (SSS-S)H WCH2 WCH3
- RITUXIMAB
- * CELLS ALONE (W/O AB)

Fig. 47

Cell surface expression of anti-human CD3 G19-4
scFv hIgG1 (SSS-S)H P238SCH2 WCH3-
hCD80TM/CT on Reh and T51 Cells.
Reh anti-CD3 (G19-4) scFv hIgG1 (SSS-S)H
P238SCH2 WCH3-hCD80TM/CT



T51 G19-4 scFv hIgG1 (SSS-S)H
P238SCH2 WCH3-hCD80TM/CT:

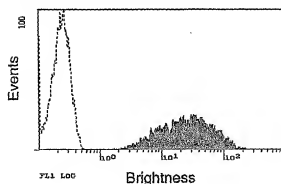
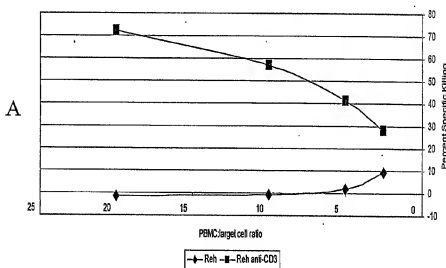


Figure 48.

Targeting of Cytotoxicity to Transfected Cell Lines by Surface expression of CD3 scFvIg

Cytotoxic activity of resting PBMC towards transfected Reh cells



Cytotoxic activity of resting PBMC towards transfected T51 lymphoblastoid cells

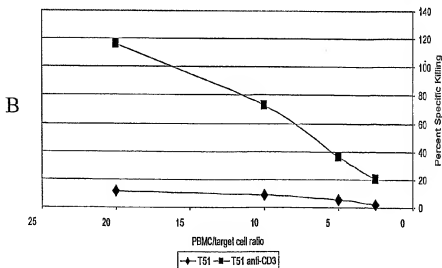
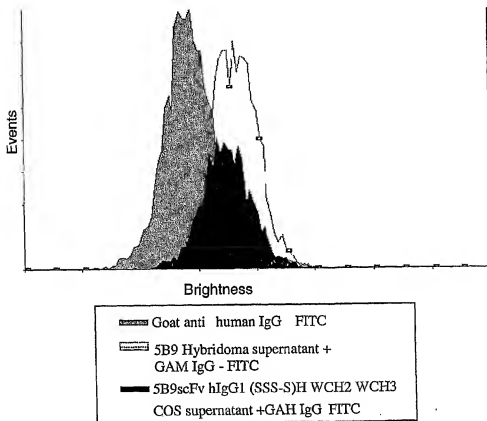


Fig. 49

Binding of 5B9, a mouse anti-human CD137 scFv hIgG1
(SSS-S)H WCH2WCH3 to stimulated human PBMC



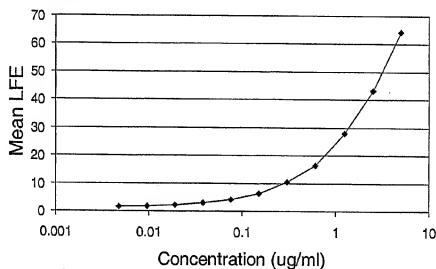
WO 2005/017148

PCT/US2003/041600

Fig. 50

Effect of V_HL11S Mutation on Cytox20
2H7 scFv hIgG1 (SSS-S)H WCH2 WCH3 Protein Expression

50A. Standard Curve: 2H7VH-L11S-IgG1 (SSS-S)H WCH2 WCH3



50B. CHO supernatant Brightness and Estimation of Protein concentrations from Standard Curve:

	CHO clone name				
	4F2	4F5	3E5	6B11A	2B8A
Mean LFE					
1/100	71.7	40.6	31.5	99.7	101.5
1/500	27.1	12.4	11.2	40.8	43
approx conc. μ g/ml	600	225	125	1000	1250

WO 2005/017148

PCT/US2003/041600

Fig. 51

Production Levels of 2H7scFv VH L11S hIgG1
(SSS-S)H WCH2 WCH3
From CHO Clone Culture Supernatants

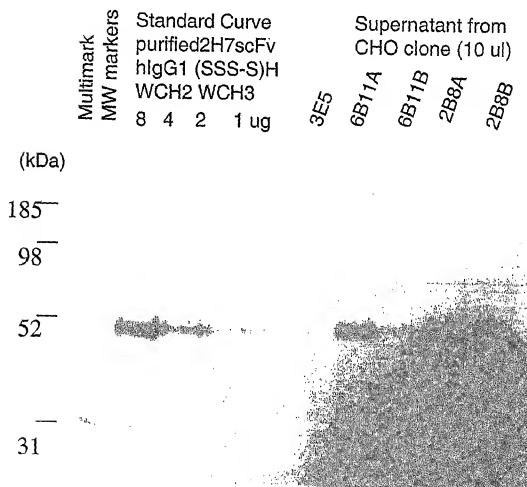
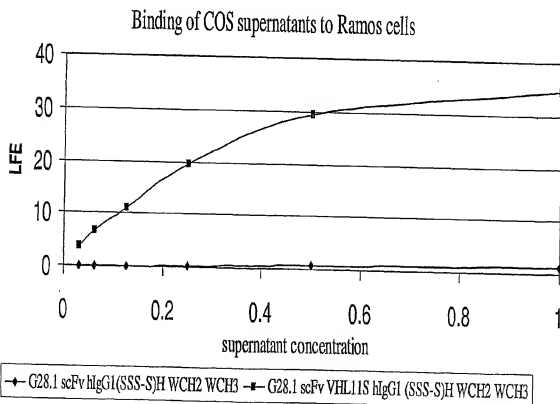


Fig. 52

Effect of VHL11S Mutation on G28-1 scFvIg Construct Protein Production from COS cells



WO 2005/017148

PCT/US2003/041600

Fig. 53

Immunoblot of G28-1 scFvIg Constructs

Increased Protein Levels in COS supernatants
transfected with G28-1scFv hlgG1 (SSS-S)H WCH2 WCH3
After Substitution of Leucine with Serine at position 11 of VH (VHL11S)

Fig. 53A.

Purified G28-1 (11/6/01)	G28-1 scFv hlgG1 (SSS-S)H	
scFv hlgG1 (SSS-S)H	WCH2 WCH3	
WCH2 WCH3	1 ul/well	
80ng		
40ng		
20ng		
10ng		
	A B C D E	

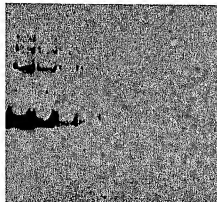


Fig. 53B.

Purified G28-1 (11/6/01)	G28-1VHL11S scFv hlgG1 (SSS-S)H	
scFv hlgG1 (SSS-S)H	WCH2 WCH3	
WCH2 WCH3	1 ul/well	
80ng		
40ng		
20ng		
10ng		
	A B C D E	

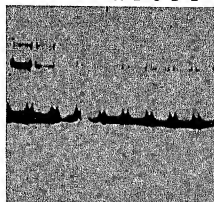


Fig. 54

Binding of 2H7 scFvIg Constructs with Altered Hinges and CH3 domains to CD20 CHO Cells

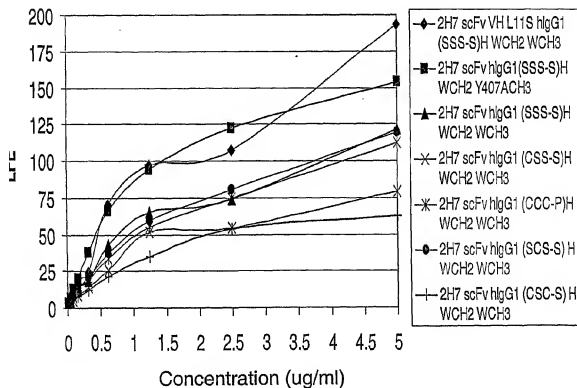


Fig. 55

ADCC Activity of 2H7 scFvlg constructs Against
BJAB Targets and PBMC Effectors

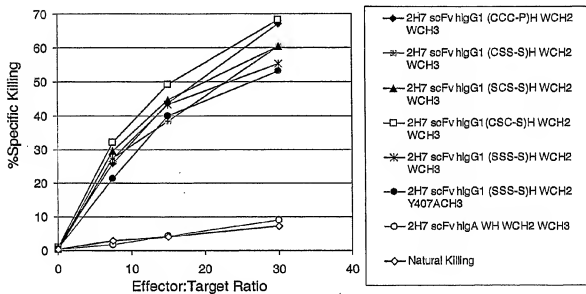
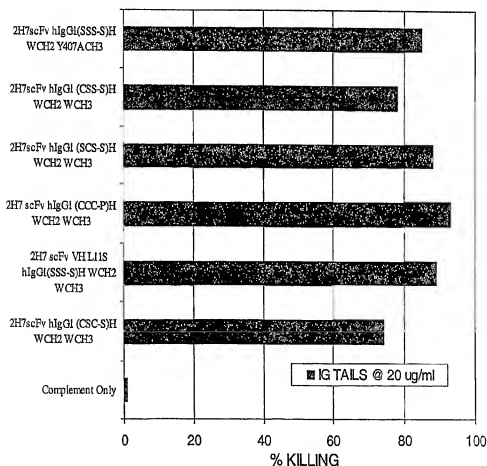


Fig. 56

Complement Activity of 2H7 scFvIg Constructs
With Ramos Target Cells



WO 2005/017148

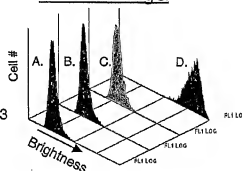
PCT/US2003/041600

Fig. 57

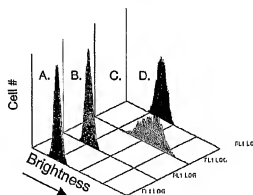
Binding of 2H7 scFvIg Derivatives to CD20CHO Cells

- A. ■ No fusion protein
B. ■ 2H7 scFv hlgE CH2CH3CH4
C. ■ 2H7 scFv hlgA WH WCH2 WCH3
D. ■ 2H7 scFv hlgG1 (SSS-S)H WCH2 WCH3

FITC anti-hlgG



FITC anti-hlgA



FITC anti-hlgE

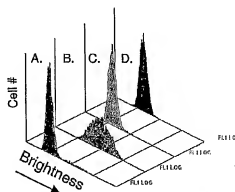


Fig. 58

Fig. 58A. 2H7 scFv VHL11S human IgE (WCH2 WCH3 WCH4)
Binding to CD20 CHO at 30 ug/ml

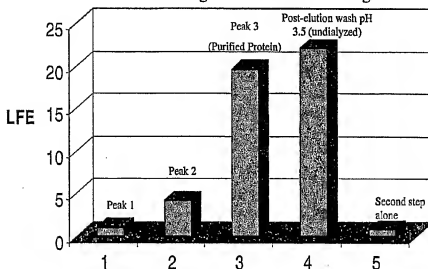
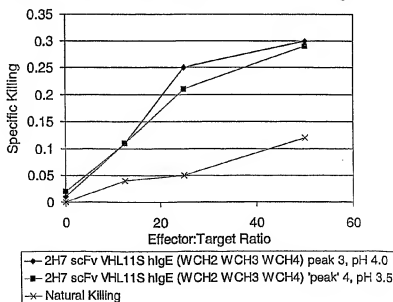


Fig. 58B. ADCC Activity of 2H7 VHL11S IgE (WCH2 WCH3 WCH4)
Protein Fractions with PBMC Effectors and Bjab Targets



WO 2005/017148

PCT/US2003/041600

Fig. 59

Binding Data for COS derived α -CD20 (2H7) scFv VHL11S
mIg E (WCH2 WCH3 WCH4) and
mIgA (WH WCH2 WCH3) Tailed Molecules

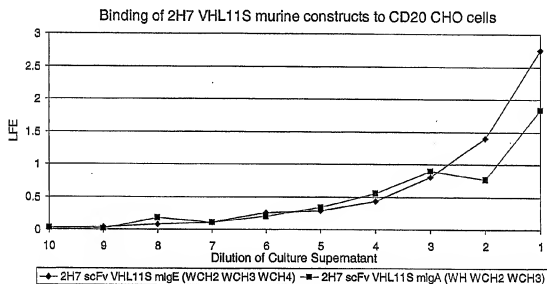
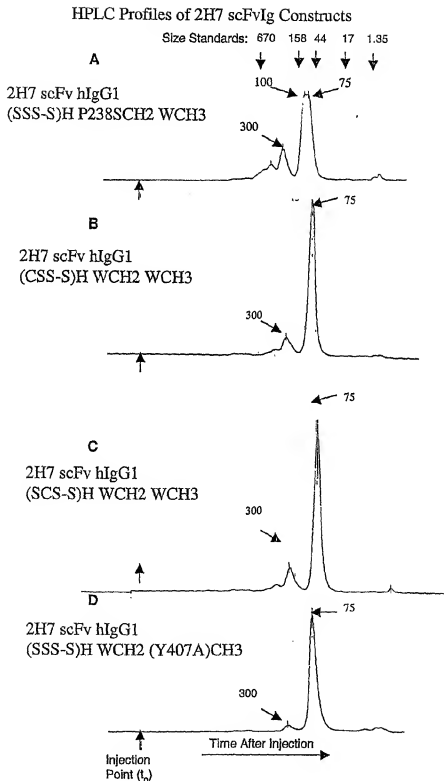


Fig. 60



WO 2005/017148

PCT/US2003/041600

Fig. 61

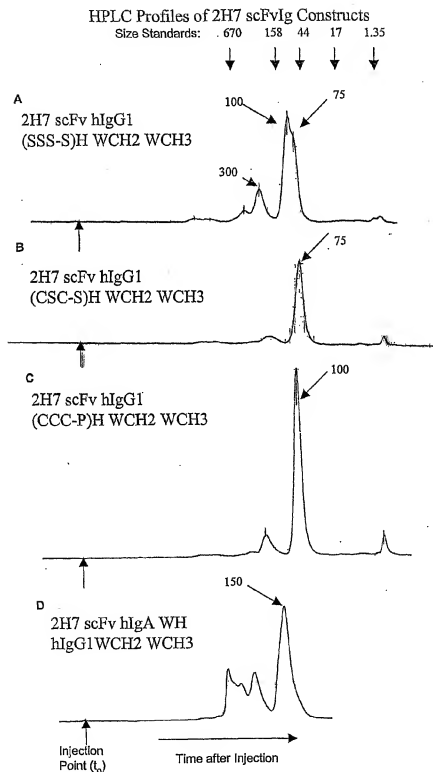


Fig. 62

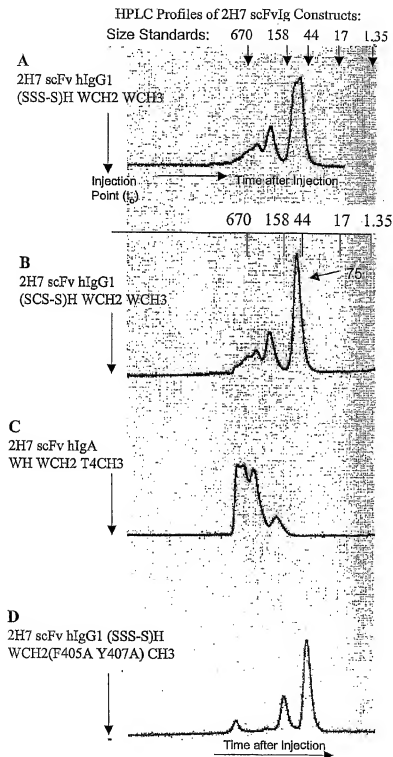


Fig. 63

Binding of Purified Proteins from COS Supernatants
to CD20 CHO cells:
Differential Effects of CH3 Mutations on Binding

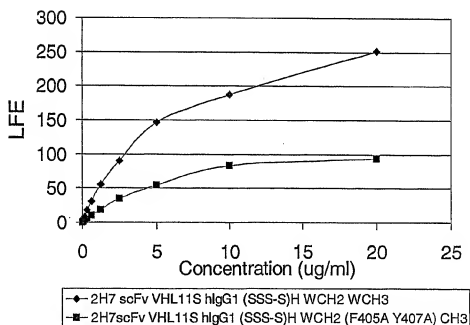
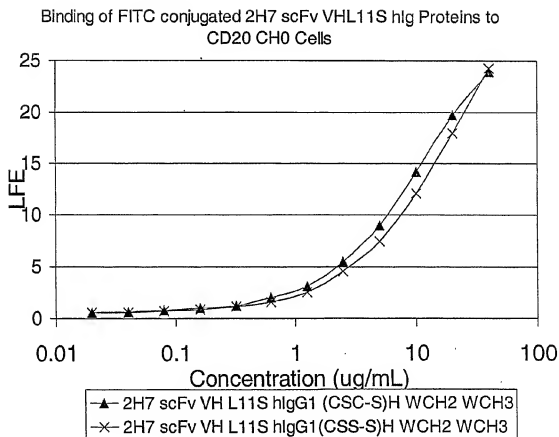


Fig. 64



WO 2005/017148

PCT/US2003/041600

Fig. 65

Nonreducing SDS-PAGE on Protein A-Purified Lots
of 2H7 scFv VHL11S hlg Constructs (10 ug/lane)

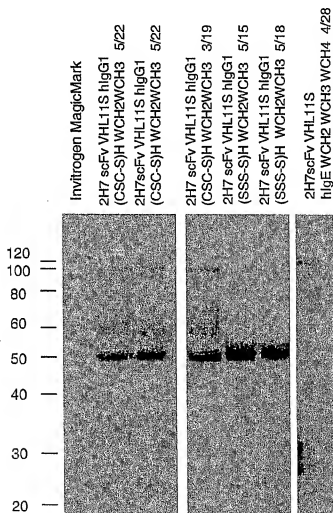


Fig. 66

Alterations in Human IgG Fc sequence
that differentially change effector function efficiency

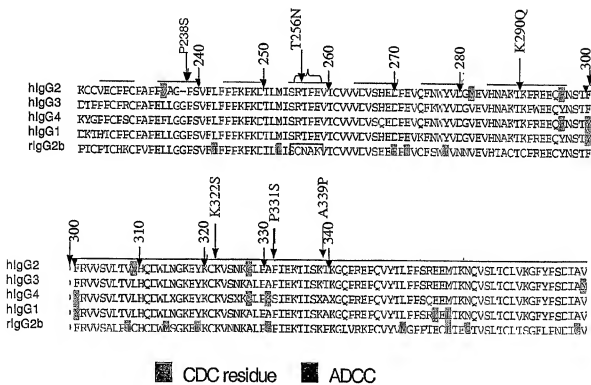


Figure 67.

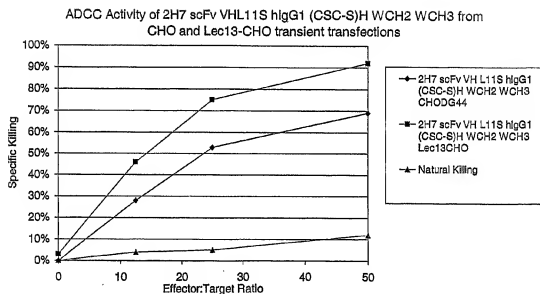
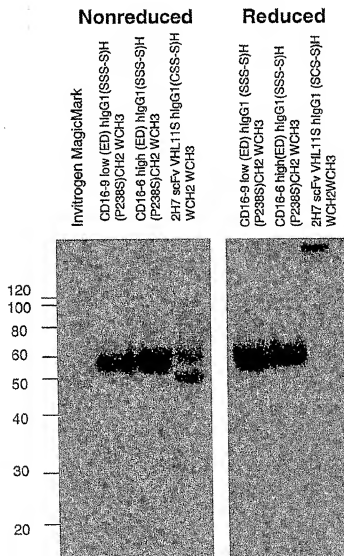


Fig. 68

CD16(ED) hlgG1(SSS-S)H P238S CH2 WCH3 high and low affinity alleles expressed as soluble molecules

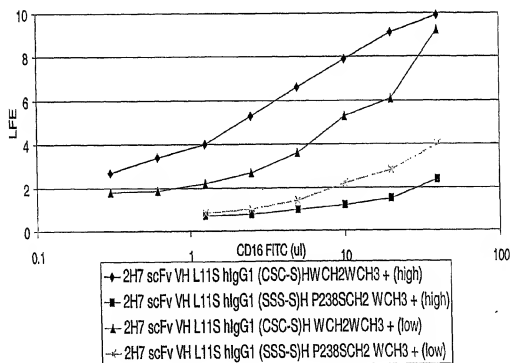


WO 2005/017148

PCT/US2003/041600

Fig. 69

Binding of soluble CD16-FITC high and low affinity fusion proteins to 2H7 scFv VHL11S hlgG1 (CSC-S)H WCH2WCH3 or (SSS-S)H (P238S)CH2WCH3 on CD20CHO Targets

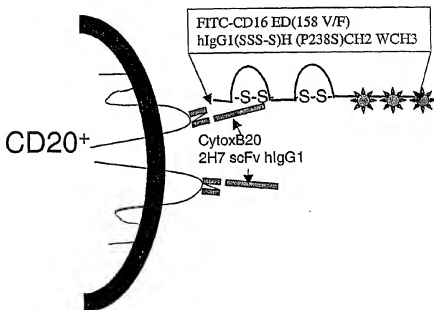


WO 2005/017148

PCT/US2003/041600

Fig. 70

Binding of FITC Labeled, Recombinant Human
CD16(ED) extracellular domain -Ig Fusion Protein to
Cytox B Derivatives on CD20 CHO Cells



Expression of surface displayed SMIPs links
modified cDNAs with the altered fusion proteins

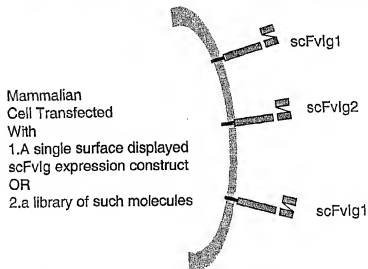


Fig. 71

CD37 mAbs and scFvIg Induce Apoptosis

scFvIg	Bjeb Staining	Annexin V Positive	
	No scFvIg	17.5	
	2H7 MH	27	
	G28-1 MH	30.6	
	G28-1 IgAH	28.9	
	HD37 MH	29.1	
	(2H7+G28-1)MH	41	
	(2H7+HD37) MH	37.1	
	(G28-1+HD37) MH	35.3	
mAbs			plus GAM
	Ramos	AnnexinV Positive	AnnexinV positive
	cells alone	3	3.3
	2H7 Mab	1.4	3.1
	G28-1 Mab	18.3	8.7
	HD37 Mab	3.7	3.1
	G28-5	3.9	8.3
	2H7+G28-1	32.3	35.7
	2H7+HD37	5	10.5
	2H7+G28-5	5.7	19.4
	HD37+G28-1	26.9	50
	HD37+G28-5	8.2	18.4
	G28-1+G28-5	39.5	68.3

WO 2005/017148

PCT/US2003/041600

Caspase 3 Activity in Ramos Cells after 4 Hour Incubation With CytotoxicB20G SMIP

media
CD20 SMIP

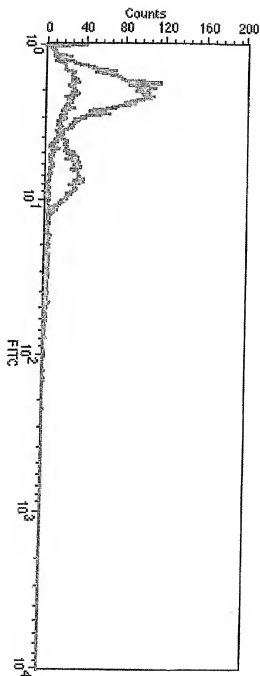


Fig. 72

Complement Dependent Cytotoxicity Mediated by CytosB20G Derivatives

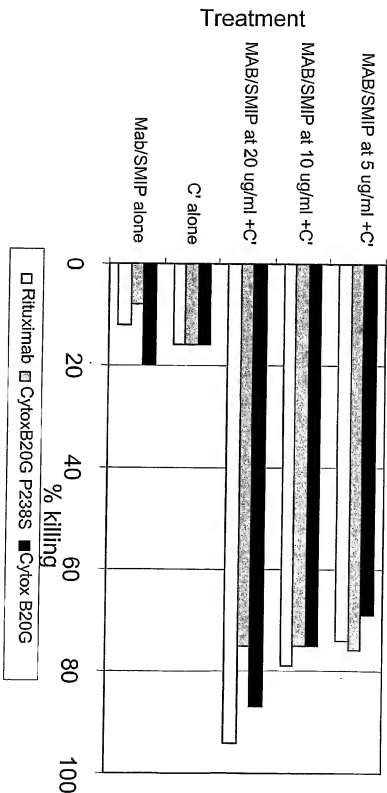


Fig. 73

Figure 76: CDC Activity of CytosB20G SMIPs. CytosB20G, CytosB20GP238, or Rituximab were incubated at increasing concentrations with 10^4 Bjab Target Cells and a 1:10 dilution of rabbit complement (Pellicrez) in a volume of 100 microliters for sixty minutes. Aliquots were stained with trypan blue (Invitrogen), and counted using a hemacytometer to determine the percentage of the cell population killed during treatment. Negative controls with cells and only one reagent were also included.

ADCC Activity of CytotoxicB20G SMIPs

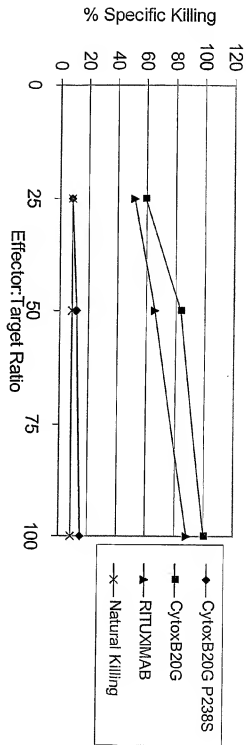


Fig. 74

Figure 77: ADCC Activity of CytotoxicB20G SMIPs. ADCC activity of CytotoxicB20G or Rituximab was measured *in vitro* against BJAB B lymphoma cell line as target and using fresh human PBMC as effector cells. Effector to target ratios were varied as follows: 100:1, 50:1, and 25:1, with the number of BJAB cells per well remaining constant but varying the number of PBMC. Bjab cells were labeled for 2 hours with ^{51}Cr and aliquoted at a cell density of 5×10^4 cells/well to each well of flat-bottom 96 well plates. Purified fusion proteins or rituximab were added at a concentration of 10 $\mu\text{g/ml}$, and PBMC were added at 1.25×10^6 cells/well (25:1), 2.5×10^6 cells/well (50:1), or 5×10^6 cells/well (100:1), in a final volume of 200 μl . Natural Killing was measured at each effector:target ratio by omission of SMIP or MAb. Spontaneous release was measured without addition of PBMC or fusion protein, and maximal release was measured by the addition of detergent (1% NP-40) to the appropriate wells. Reactions were incubated for 5 hours, and 100 μl culture supernatant harvested to a Lunaplate (Packard Instruments) and allowed to dry overnight prior to counting cpm released on a Packard Top Count NXT Microplate Scintillation Counter.

WO 2005/017148

PCT/US2003/041600

Binding of soluble FITC-CD16 to Cytox20G on CD20 CHO Cells

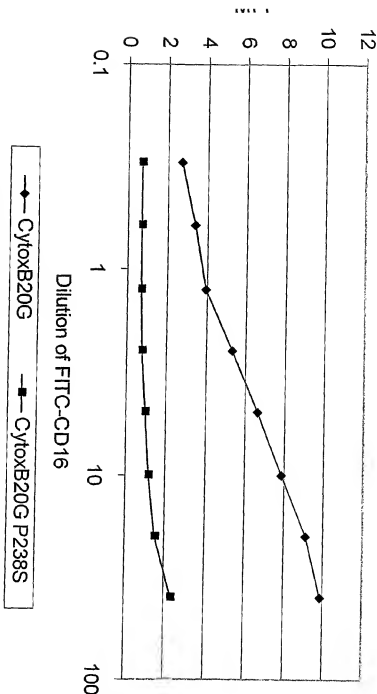


Fig. 75

re 78: Binding of soluble FITC-CD16 to Cytox20G on CD20 CHO cells. CD20 CHO cells (10^6) were incubated with saturating amounts of Cytox20G or Cytox20G P238S (10 μ g/ml) for one hour on ice in PBS/2% FBS. Cells were washed in PBS/2% FBS and incubated with serial dilutions of 0.5 μ g/ml FITC-CD16 for one hour on ice. Cells were washed and specific binding measured by flow cytometry using a Beckman-Coulter Epics C machine. Results were analyzed using Expo analysis software and normalized fluorescence units graphed as a function of concentration.

CytoxB20G and CytoxB20G P238S SMIPs bind to U937 Cells Expressing FcγRI High Affinity FcR

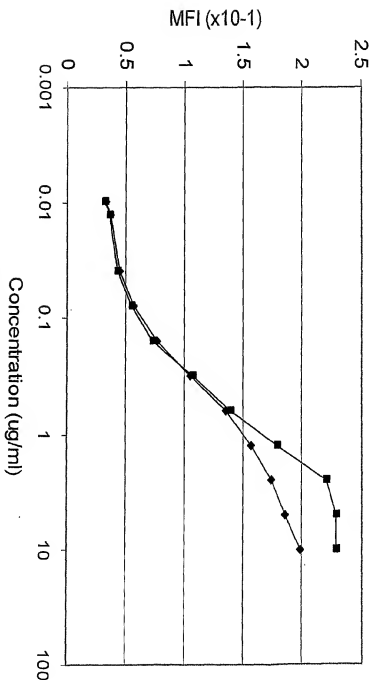


Fig. 76

re 79: CytoxB20G SMIPs bind similarly to U937 cells expressing the high affinity FcR (FcγRI, CD64). U937 cells expressing CD64 were incubated in PBS/2%FBS for one hour on ice with CytoxB20G or CytoxB20G P238S. Cells were washed and incubated for one hour on ice with FITC-goat anti-human IgG1 (Fc specific) (Caltag) at a final dilution 100. Cells were washed and fluorescence analysed on a Beckman-Coulter Epiflow cytometer. Data was analyzed using Expo analysis software, and fluorescence intensity graphed as a function of SMIP concentration.

B Cell Depletion Mediated by CytoxB20G SMIPs

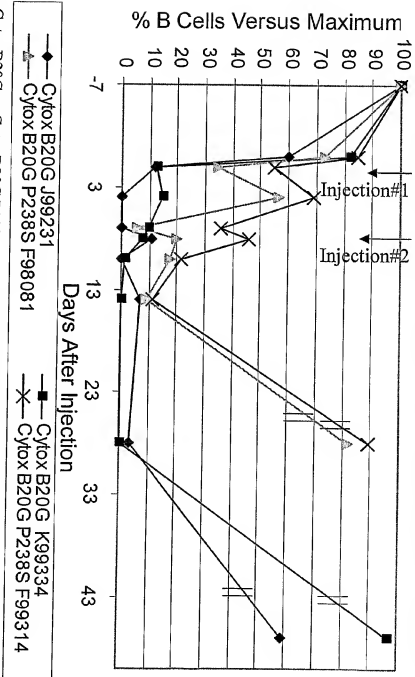


Fig. 77

10: CytoxB20G or CytoxB20G P238S were administered to macaques by intravenous injection at 6 mg/kg, with injections given one week apart. The effect on circulating B cells was measured by detection of CD40 positive B cells in peripheral blood. Blood samples were drawn from injected animals at days -7, 0, 1, 3, 7, 8, 10, 14, 28, and 43. B cell number was estimated by performing CBC (complete blood counts) and two color flow cytometry analysis on monkey FITC or PE conjugates of antibodies against CD40, CD19, CD20, IgG, CD3, CD8 were used in various experiments. Data are plotted as the number of CD40 positive blood B cells tabulated in thousands of cells per μ l over time relative to the initial pre-injection time point level of B cells (maximum).

WO 2005/017148

PCT/US2003/041600

Figure 81: SEC on Cytox37G SMIPs containing SSS and SSC hinge Domains from Human IgG1

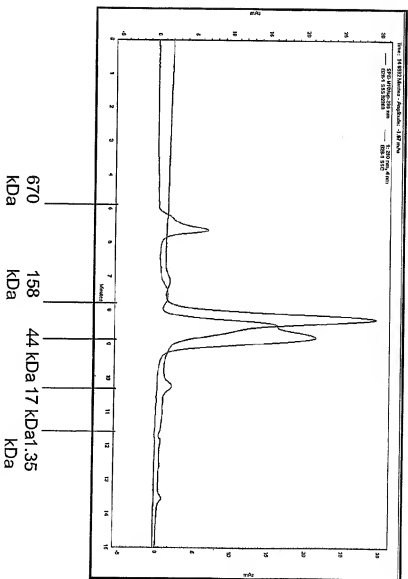


Fig. 78

Figure 81: SEC (Size Exclusion Chromatography) Cytox37G SMIPs were purified from CHO culture supernatants by Protein A affinity chromatography. Purified aliquots of 10-25 μ g were subjected to HPLC over a Tosoh Biosep, Inc. TSK 3000 SWXL HPLC column, pore size 5 μ m. The flow rate was 1 ml/min, in PBS, pH 7.2 running buffer. Migration rates of molecular weight standards are indicated below the tracing. The Cytox37G (SSS)H SMIP indicated in blue, while the Cytox37G (CSS)H is indicated in red.

Figure 82: Binding of CytoxB37G SMIPs to B Cell Lymphoma Cell Lines

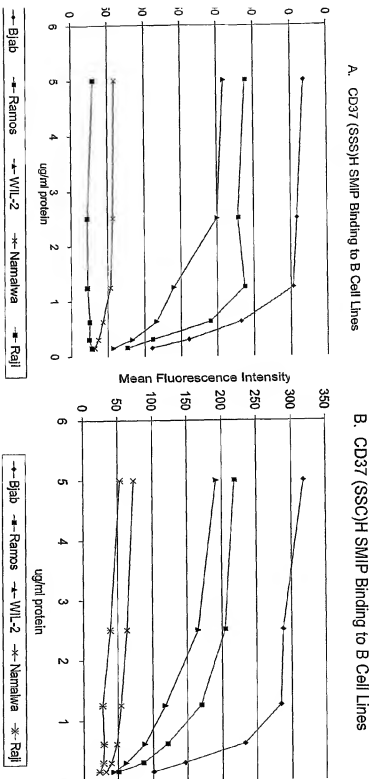


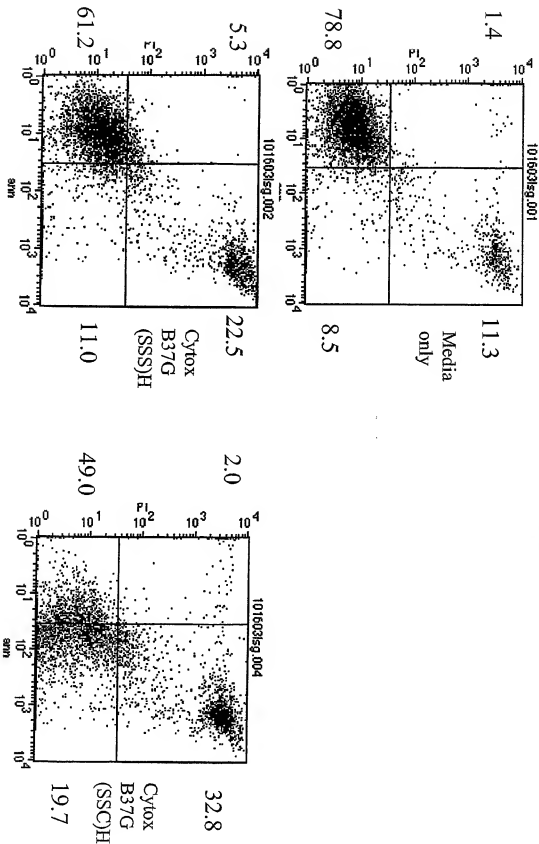
Fig. 79

ure 82: Binding of CytoxB37G SMIPs to B cell lymphoma cell lines. Serial dilutions of ified CytoxB37 (SSS)H G or CytoxB37 (SSC)H G SMIPs were incubated with 10^6 cells of each cell type for 60 minutes on ice in PBS/2%FBS. Samples were washed twice, and incubated with a mixture of FITC goat anti-human ; and FITC goat anti-human IgG F(ab')₂ (CalTag) at 1:100 each, on ice for 45 minutes. Samples were washed and lyzed by flow cytometry using a FACScalibur (Becton-Dickinson)

WO 2005/017148

PCT/US2003/041600

Fig. 80: AnnexinV-PI Staining of Ramos Cells Incubated
24 hours with CD37 SMIPs



WO 2005/017148

PCT/US2003/041600

Figure 84: Thymidine Incorporation (Growth Inhibition) in Ramos B-cells after a 48 Hour Incubation with anti-CD37 SMIPs

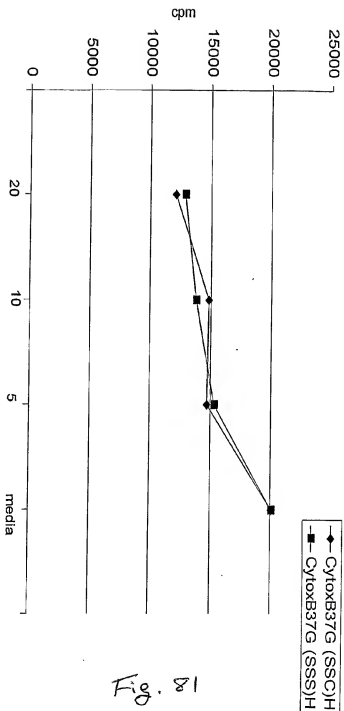


Fig. 81

Example 84: Ramos B cells were incubated with serial dilutions of purified CD37G SMIPs containing or the IgG1 hinge identified as (SSS)H or (SSC)H. Cultures were incubated in 96 well flat bottom culture dishes (Costar) at 37°C, 5%CO₂ for 36 hours prior to pulsing with ³H-thymidine for the 12 hours of a 48 hour incubation (0.75 µCi/well). Cells were harvested onto 96-well GFC plates e.g. a Packard harvester, dried, and 25 µl Microscint scintillation fluid added to each well prior to counting on a TopCount NXT microplate (Packard) scintillation counter. Data are plotted as cpm reported versus protein concentration. Each SMIP show increasing inhibition of proliferation with increasing protein concentration.

Figure 85: The Induction of Apoptosis in Ramos B-cells after a 20 hour incubation with different combinations of CD20 and CD37 targeted SMIPs

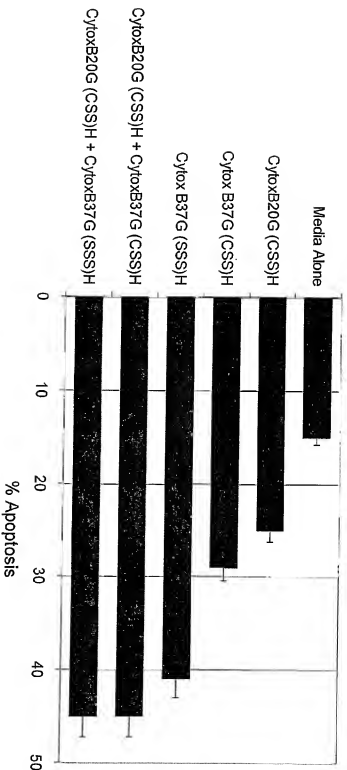


Fig. 82

Figure 85: Ramos B cells were incubated with CD20 and/or CD37 targeted SMIPs (10 /ml) in solution for 20 hours. Cells were then harvested, washed, and incubated in annexin V and propidium iodide using a staining kit from Immunotech prior to two color flow cytometry using a FACScalibur flow cytometer (Becton-Dickinson). The graph shows the percentage of annexin V positive cells identified by their staining in the right quadrants of the dot plots.

Figure 86: Complement Mediated Killing of Ramos Cells by CD37 SMIPs

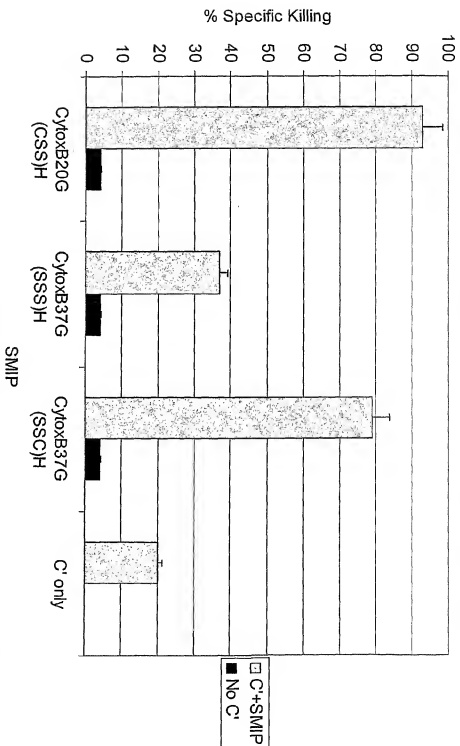


Fig. 83

Figure 86: CDC Activity of CytoxB37G SMIPs. CytoxB20G, CytoxB37 (SSS)H G, CytoxB37 (SCS)H, CytoxB37 (CSS)H, or CytoxB37 (SSC)H were incubated at 10 μ g/ml with 10^4 Ramos Target Cells and a 1:10 dilution of rabbit complement (PelFreez) in a volume of 150 μ l for 90 minutes. Aliquots were stained with trypan blue (Invitrogen), and counted using a hemacytometer to determine the percentage of the cell population killed during treatment. Negative controls with cells and only one reagent were also included.

Figure 87: ADCC Activity of CD37 SMIPs Against Ramos Targets

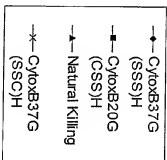
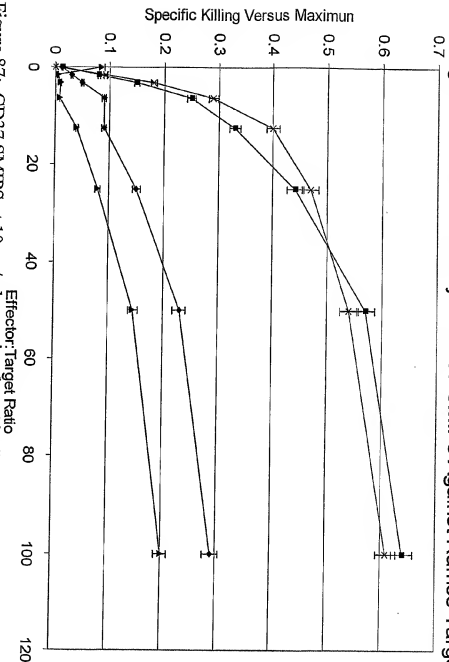


Fig. 84

Figure 87: CD37 SMIPs at 10 $\mu\text{g/ml}$ were incubated in flat-bottom 96 well plates with 10^4 ^{51}Cr -labeled Ramos cells and resting human PBMCs at different effector:target ratios ranging from 0 to 100. All incubations were performed in triplicate at each effector:target ratio. Natural Killing was measured at each effector:target ratio by omission of SMIP. Spontaneous release was measured without addition of PBMC or fusion protein, and maximal release was measured by the addition of detergent (1% NP-40) to the appropriate wells. Reactions were incubated for 6 hours, and 100 μl culture supernatant harvested to a Lumaplate (Packard Instruments) and allowed to dry overnight prior to counting cpm released on a Packard Top Count NXT Microplate Scintillation Counter.

INTERNATIONAL SEARCH REPORT

International application No.

PCT/US03/41600

A. CLASSIFICATION OF SUBJECT MATTER IPC(7) : C12N 15/00; A61K 39/395; C07K 16/00 US CL : 530/387.3, 388.85, 391.3; 424/130.1; 536/23.4; 435/320.1, 69.6 According to International Patent Classification (IPC) or to both national classification and IPC		
B. FIELDS SEARCHED Minimum documentation searched (classification system followed by classification symbols) U.S. : 530/387.3, 388.85, 391.3; 424/130.1; 536/23.4; 435/320.1, 69.6 Documentation searched other than minimum documentation to the extent that such documents are included in the fields searched Electronic data base consulted during the international search (name of data base and, where practicable, search terms used) Please See Continuation Sheet		
C. DOCUMENTS CONSIDERED TO BE RELEVANT		
Category *	Citation of document, with indication, where appropriate, of the relevant passages	Relevant to claim No.
Y	HAYDEN et al. Single-chain mono- and bispecific antibody derivatives with novel biological properties and antitumor activity from COS cell transient expression system. Therapeutic Immunology. 1994, Vol. 94, pages 3-15, especially Figure 1, Methods.	1-7, 20-28, 31-40, 53-57, 59, 62-63, 65-75, 116-119, 129-137, 140-150, 161-169, 171-181, 238, 240-243, 251-259, 261-267, 282-285, 287-295, 399-411
Y	US 6,147,203 A (PASTAN et al.) 14 November 2000 (14.11.2000), see entire document, especially abstract, column5-6.	1-7, 20-28, 31-40, 53-57, 59, 62-63, 65-75, 116-119, 129-137, 140-150, 161-169, 171-181, 238, 240-243, 251-259, 261-267, 282-285, 287-295, 399-411
<input checked="" type="checkbox"/> Further documents are listed in the continuation of Box C. <input type="checkbox"/> See patent family annex.		
* Special categories of cited documents: "A" documents defining the general state of the art which is not considered to be of particular relevance "E" earlier application or patent published on or after the international filing date "L" document which may throw doubts on priority claim(s) or which is cited to establish the publication date of another citation or other special reason (as specified) "O" document referring to an oral disclosure, use, exhibition or other means "P" document published prior to the international filing date but later than the priority date claimed	"T" later document published after the international filing date or priority date and not in conflict with the application but cited to understand the principle or theory underlying the invention "X" document of particular relevance; the claimed invention cannot be considered novel or cannot be considered to involve an inventive step when the document is taken alone "Y" document of particular relevance; the claimed invention cannot be considered to involve an inventive step when the document is combined with one or more other such documents, such combination being obvious to a person skilled in the art "&" document member of the same patent family	
Date of the actual completion of the international search 29 October 2004 (29.10.2004)		Date of mailing of the international search report 02 NOV 2004
Name and mailing address of the ISA/US Mail Stop PCT, Attn: ISA/US Commissioner for Patents P.O. Box 1450 Alexandria, Virginia 22313-1450 Facsimile No. (703) 305-3230		Authorized officer Eric R. Helms Telephone No. 571-272-1600

INTERNATIONAL SEARCH REPORT

PCT/US03/41600

C. (Continuation) DOCUMENTS CONSIDERED TO BE RELEVANT

Category *	Citation of document, with indication, where appropriate, of the relevant passages	Relevant to claim No.
Y	US 6,074,644 A (PASTAN et al.) 13 June 2000 (13.06.2000), see entire document, especially column 20.	26, 28, 32, 135, 137, 142, 257, 259, 262
Y	US 5,677,425 A (BODMER et al.) 14 October 1997 (14.10.1997), see entire document, especially abstract, column 3-4.	65-75, 116, 172-180, 288-295
Y	US 6,482,919 B2 (LEDBETTER et al.) 19 November 2002 (19.11.2002), see entire document.	180

INTERNATIONAL SEARCH REPORT

PCT/US03/41600

Continuation of B. FIELDS SEARCHED Item 3:

CAPLUS, MEDLINE, WEST, BIOSIS

Search terms: inventor name, scfv, hinge, cysteine, fusion protein, CD19, CD3, deleted hinge, altered hinge, IgG1, IgA, IgE, disulfide stabilized, constnat region.